COMMUNICATIONS: SIF Congress 2013

Properties of the Higgs-like boson in the $H \to ZZ \to 4\ell$ decay channel at CMS

L. FINCO

INFN, Sezione di Torino - Torino, Italy

Summary. — The measurement of the properties of the new boson with mass around 126 GeV are reported. The analysis uses pp collision data recorded by the CMS detector at the LHC, corresponding to integrated luminosities of $5.1\,\mathrm{fb}^{-1}$ at $\sqrt{s} = 7\,\mathrm{TeV}$ and $19.6\,\mathrm{fb}^{-1}$ at $\sqrt{s} = 8\,\mathrm{TeV}$. The boson is observed in the $H \to ZZ \to 4\ell$ channel ($\ell = e, \mu$) with a local significance above the expected background of 6.8 standard deviations. The mass is measured to be $125.6 \pm 0.4(\mathrm{stat.}) \pm 0.2(\mathrm{syst.})\,\mathrm{GeV}$. The spin-parity of the boson is studied and the pure scalar hypothesis is found to be consistent with the observation, when compared to the other spin-parity hypotheses. No other significant Standard Model Higgs-like excess is found in the search and upper limits at 95% confidence level exclude the range 129.5–832.0 GeV.

PACS `14.80.Bn` – Standard-model Higgs bosons.

This article describes the study of the properties of the Higgs-like particle (H) discovered in July 2012 by the CMS and ATLAS collaborations [1,2], in the $H \to ZZ$ decay channel, where both Z bosons decay to lepton pairs. The proton-proton collision data used in this analysis were recorded by the Compact Muon Solenoid (CMS) detector at the Large Hadron Collider (LHC) and correspond to integrated luminosities of $5.1\,\mathrm{fb}^{-1}$ at $\sqrt{s} = 7\,\mathrm{TeV}$ and $19.6\,\mathrm{fb}^{-1}$ at $\sqrt{s} = 8\,\mathrm{TeV}$. After a brief overview of the analysis strategy, the kinematic discriminant and the event categorization based on jet multiplicity are introduced, being fundamental tools of the event selection and kinematics. The Higgs-like properties, *i.e.* significance, signal strength, mass and spin-parity quantum numbers, are then examined.

The $H \to ZZ \to 4\ell$ analysis [3] is based on the reconstruction, identification and isolation of leptons. Each signal event consists of two pairs of same-flavor and opposite-charge leptons in the final state, isolated and with high transverse momentum, and it is compatible with a ZZ system, where one or both Z bosons can be off-shell. The sources of background for the $H \to ZZ \to 4\ell$ channel are the irreducible four-lepton contribution from direct ZZ (or $Z\gamma^*$) production, very similar to the signal, the reducible background arising from $Zb\bar{b}$ and $t\bar{t} \to 4\ell$ decays and the instrumental contribution
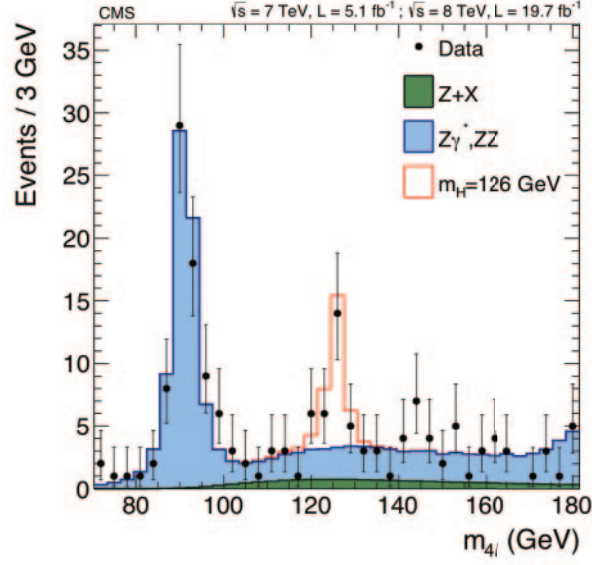
Fig. 1. – Distribution of the four-lepton reconstructed mass. Points represent the data, shaded histograms represent the background and the unshaded histogram the signal expectation for a mass hypothesis of $m_H = 126$ GeV.

due to a misidentification of the leptons. In fig. 1 the distribution of the four-lepton reconstructed mass is reported, for both data and Monte Carlo (MC) samples.

In order to separate signal from background events, a kinematic discriminant is defined ($\mathcal{D}_{bkg}^{kin}$), depending on the five production and decay angles $\vec{\Omega} \equiv (\theta^*, \Phi_1, \theta_1, \theta_2, \Phi)$ and the Z boson masses (fig. 2). These variables fully describe the event topology and have a
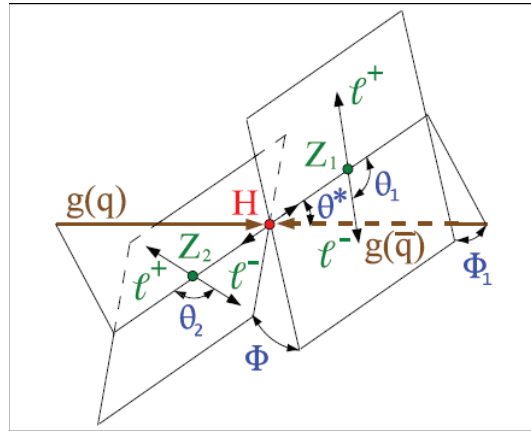

Fig. 2. – Illustration of the production and decay of a particle H $gg(q\bar{q}) \rightarrow H \rightarrow Z_1 Z_2 \rightarrow 4\ell$ with the two production angles θ^* and Φ_1 shown in the H rest frame and three decay angles θ_1, θ_2, and Φ shown in the Z_i and H rest frames, respectively.
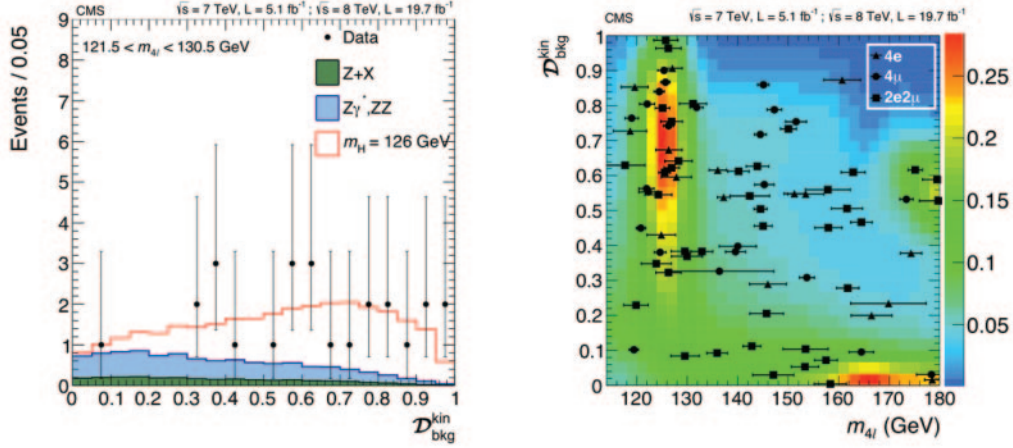
Fig. 3. – Distribution of the kinematic discriminant $\mathcal{D}_{bkg}^{kin}$ for events in the mass region $121.5 < m_{4\ell} < 130.5$ GeV (left). Distribution of the kinematic discriminant $\mathcal{D}_{bkg}^{kin}$ *versus* the four-lepton reconstructed mass $m_{4\ell}$ (right) with contours shown for the expected relative density of signal events for $m_H = 126$ GeV. The points show the data with measured invariant mass uncertainties as horizontal bars.

high discriminating power. The $\mathcal{D}_{bkg}^{kin}$ discriminant [4] is based on the probability ratio of the signal and background hypotheses and it is defined as

$$\mathcal{D}_{bkg}^{kin} = \frac{\mathcal{P}_{sig}^{kin}}{\mathcal{P}_{sig}^{kin} + \mathcal{P}_{bkg}^{kin}},$$

where $\mathcal{P}^{kin}$ is the probability distribution of angular and mass observables $(\vec{\Omega}, m_{Z_1}, m_{Z_2})$. $\mathcal{D}_{bkg}^{kin}$ is thus constrained to be between 0 and 1. In fig. 3 (left) the one-dimensional distribution of the kinematic discriminant is plotted in the $m_{4\ell}$ interval of the Higgs peak, for both MC and data samples. The distribution of the $\mathcal{D}_{bkg}^{kin}$ *versus* the four-lepton reconstructed mass $m_{4\ell}$ is shown in fig. 3 (right) in the low mass range and it is compared to the Standard Model (SM) signal expectation for $m_H = 126$ GeV. A signal-like clustering of events is apparent at high values of $\mathcal{D}_{bkg}^{kin}$ around $m_{4\ell} \sim m_H$.

In order to have an optimal sensitivity to the different production mechanisms, a categorization based on the jet multiplicity is introduced. The event sample is thus split into two categories, depending on the number of jets: the *0/1-jet* category is formed of events with fewer than two jets, while the *dijet* one is composed of events with at least two jets. Two discriminants are then defined, according to the category. In the *0/1-jet* sample the transverse momentum of the four-lepton system ($p_T^{4\ell}$) is used to discriminate vector boson fusion (VBF) and the associated Higgs production with a W/Z boson (VH) from gluon fusion. In the other category a linear discriminant ($\mathcal{D}_{jet}$) is formed combining two VBF sensitive variables. In the *0/1-jet(dijet)* category, about 5 (20%) of the signal events are expected to come from VBF production mechanism. The distributions of the $p_T^{4\ell}$ and $\mathcal{D}_{jet}$ discriminants are reported in fig. 4.

The mass measurement of the analyzed particle is performed with a three-dimensional fit using for each event the four-lepton invariant mass ($m_{4\ell}$), the associated per-event
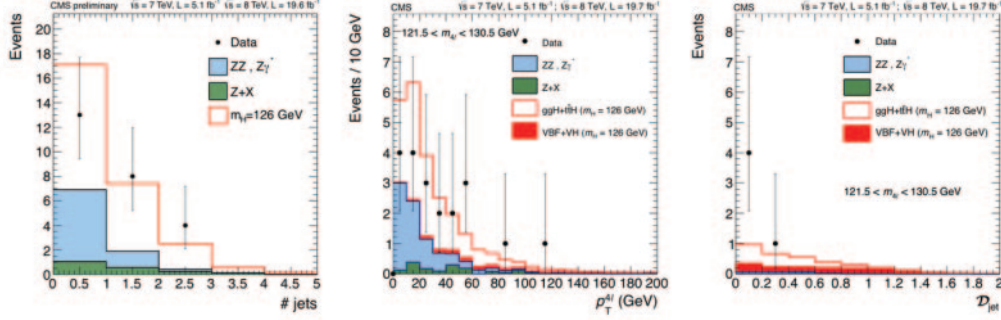
Fig. 4. – Distribution of the number of jets (left). Distribution of $p_T^{4\ell}$ in the *0/1-jet* category (center). Distribution of the $\mathcal{D}_{jet}$ discriminant in the *dijet* category (right). Only events in the mass region $121.5 < m_{4\ell} < 130.5$ GeV are considered.

mass error ($\mathcal{D}_m$) and the kinematic discriminant ($\mathcal{D}_{bkg}^{kin}$). Per-event errors on the four-lepton invariant mass are calculated from the individual lepton mass errors and including them in the fit allows to gain 8% improvement in the Higgs boson mass measurement uncertainty. Figure 5 shows the likelihood scan as a function of mass, depending on which variables are used as input of the fit (left) and dividing the three different final states, 4μ, $4e$ and $2\mu 2e$ (right). The fit procedure gives $m_H = 125.6 \pm 0.4(\text{stat.}) \pm 0.2(\text{syst.})$ GeV and the CMS result in this channel is the most precise Higgs mass measurement ever achieved.

The other properties of the new resonance are extracted performing a multi-dimensional likelihood fit that depends on the $\mathcal{D}_{bkg}^{kin}$ and $\mathcal{D}_{jet}$ (or $p_T^{4\ell}$) discriminants and on the four-lepton reconstructed mass $m_{4\ell}$ of each event. The minimum of the local p-value, *i.e.* the significance of local excesses relative to the background expectation, is obtained from the fit procedure and it is reached at $m_{4\ell} = 125.7$ GeV. This value
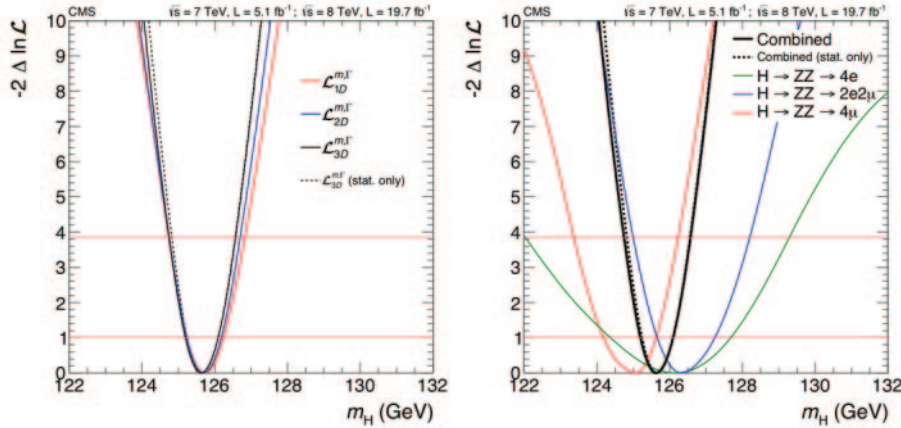

Fig. 5. – Likelihood scan as a function of mass for 1D ($m_{4\ell}$), 2D ($m_{4\ell}, \mathcal{D}_m$) and 3D ($m_{4\ell}, \mathcal{D}_m, \mathcal{D}_{bkg}^{kin}$) analysis (left). Likelihood scan as a function of mass obtained from the 3D test statistics for the different final states and their combination (right).
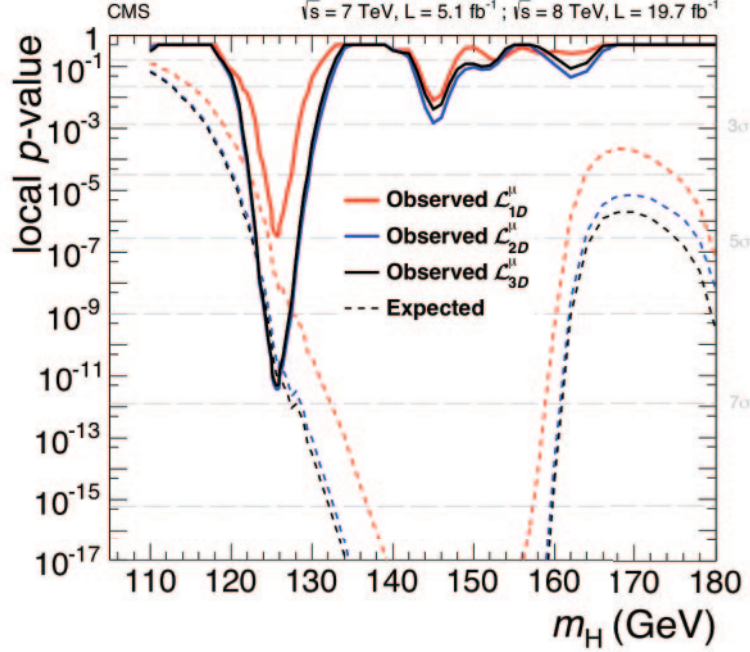
Fig. 6. – Significance of the local excess with respect to the SM background expectation as a function of the Higgs boson mass in the low-mass range. The dashed line shows the mean expected significance of the SM Higgs signal for a given mass hypothesis. Red is the 1D model ($m_{4\ell}$), blue is the 2D model ($m_{4\ell}$, $\mathcal{D}_{bkg}^{kin}$) and black is the 3D model ($m_{4\ell}$, $\mathcal{D}_{bkg}^{kin}$, $\mathcal{D}_{jet}$ or $p_T^{4\ell}$).

corresponds to a local significance of 6.8σ (for an expectation of 6.7σ) and it constitutes the observation of the new boson in the four-leptons channel alone. This is the only significant excess in the range $m_H < 1\,\mathrm{TeV}$. The p-value distribution is shown for the low mass range as a function of m_H in fig. 6.

The parameter that describes the magnitude of the Higgs signal is the signal strength modifier, defined as the ratio of the observed cross section and the cross section predicted by the SM ($\mu = \sigma_{obs}/\sigma_{SM}$). The measured value of μ is obtained using the full 3D model introduced in the previous paragraph and, at the best fit mass ($m_H = 125.6\,\mathrm{GeV}$), it is

$$\mu = 0.93^{+0.26}_{-0.23}(\text{stat.})^{+0.13}_{-0.09}(\text{syst.}).$$

The signal strength is also calculated in each jet category separately:

$$\mu_{0/1-jet} = 0.83^{+0.31}_{-0.25},$$
$$\mu_{dijet} = 1.45^{+0.89}_{-0.62}.$$

A visualization of the signal strength fits is presented in fig. 7 (left). Both categories are compatible with the combined value and with the expected cross section by the SM ($\mu = 1$).

In addition, one can introduce two other signal strength modifiers, sensitive to fermion (gluon fusion, $t\bar{t}H$) or vector boson (VBF, VH) production. A 2D fit is thus performed
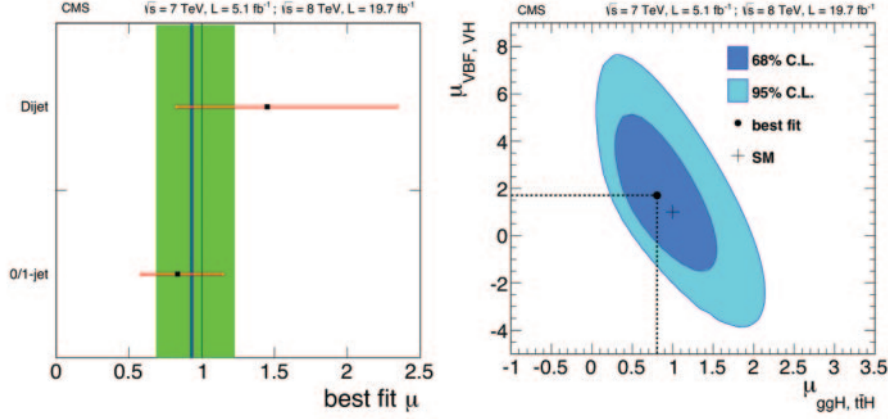
Fig. 7. – Values of $\mu = \sigma_{obs}/\sigma_{SM}$ for the two categories (left). The vertical line shows the combined μ, together with its associated $\pm1\sigma$ uncertainties shown as green band. The horizontal bars indicate the $\pm1\sigma$ uncertainties in μ for the different categories. The uncertainties include both statistical and systematic contributions. Likelihood contours on the signal strength modifiers associated with fermions ($\mu_{ggH,t\bar{t}H}$) and vector bosons ($\mu_{VBF,VH}$) shown at 68% and 95% confident level (right).

in order to give the allowed region for $(\mu_{ggH,t\bar{t}H}, \mu_{VBF,VH})$ and at 125.6 GeV it yields

$$\mu_{ggH,t\bar{t}H} = 0.80^{+0.46}_{-0.36},$$
$$\mu_{VBF,VH} = 1.7^{+2.2}_{-2.1}.$$

The fit result is reported in fig. 7 (right).

In order to determine the spin and the parity of the new boson, a methodology with kinematic discriminants is used, as in the D^{kin}_{bkg} approach. Two discriminants are defined:

$$\mathcal{D}_{JP} = \frac{\mathcal{P}_{SM}}{\mathcal{P}_{SM} + \mathcal{P}_{JP}},$$

where $\mathcal{P}_{SM}$ is the probability distribution for the SM Higgs boson (0^+) hypothesis and $\mathcal{P}_{JP}$ is the probability for an alternative model, and

$$\mathcal{D}_{bkg} = \frac{\mathcal{P}_{SM}}{\mathcal{P}_{SM} + \mathcal{P}_{bkg}},$$

where $\mathcal{P}_{bkg}$ is the probability distribution for the background ($\mathcal{D}_{bkg}$ extends $\mathcal{D}^{kin}_{bkg}$, using also the four-lepton mass probability). The first observable thus emphasizes separation of the SM Higgs boson hypothesis from an alternative signal hypothesis and the second one discriminates signal from background. In fig. 8 (left) the $\mathcal{D}_{bkg}$ distribution is shown, in the mass range $106 < m_{4\ell} < 141$ GeV: this distribution is very similar between the SM and alternative signal hypotheses, but differs significantly from background. The $\mathcal{D}_{0^-}$ behavior is plotted in fig. 8 (center) in the same mass range, as an example.
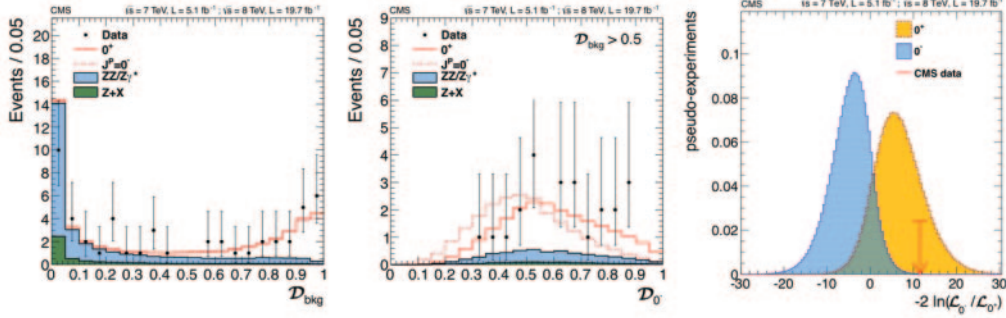
Fig. 8. – Distribution of $\mathcal{D}_{bkg}$ in data and MC expectations for the background and for a signal resonance consistent with SM Higgs boson at $m_H = 125.6\,\text{GeV}$ (left). Distribution of $\mathcal{D}_{0^-}$ with a requirement $\mathcal{D}_{bkg} > 0.5$, where data (points with error bars) and expectations for background and signal are shown (center). Distribution of $q = -2\ln(\mathcal{L}_{JP}/\mathcal{L}_{SM})$ for two signal types (0^+ represented by the yellow histogram and 0^- hypothesis by the blue histogram) for $m_H = 126\,\text{GeV}$ shown with a large number of generated experiments (right); the arrow indicates the observed value.

The distribution of the test statistic $q = -2\ln(\mathcal{L}_{JP}/\mathcal{L}_{SM})$ is defined using the ratio of signal-plus-background likelihoods for two signal hypotheses ($\mathcal{L}_i$) and it is examined with generated samples for $m_H = 125.6\,\text{GeV}$. Results are summarized in table I and in fig. 9. The expected distributions of q for the pseudoscalar hypothesis and the SM Higgs boson are shown in fig. 8 (right) and the observed value of the test statistic is indicated by the red arrow. A confidence levels (CLs) criterion is defined as the ratio of the probabilities to observe, under the J^P and 0^+ hypotheses, a value of the test statistic q equal or larger than the one in the data. The data disfavor the alternative hypotheses J^P with a CLs value in the range 0.001–10%.

TABLE I. – *List of models used in analysis of spin-parity hypotheses and corresponding CLs values.*

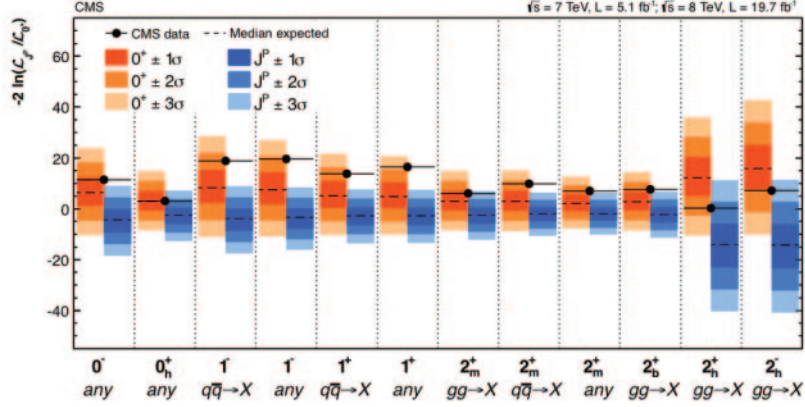| J^P model	J^P production	CLs (%)
0^-	any	0.09
0_h^+	any	7.1
1^-	$q\bar{q} \to X$	0.001
1^-	any	0.001
1^+	$q\bar{q} \to X$	0.03
1^+	any	0.01
2_m^+	$gg \to X$	1.9
2_m^+	$q\bar{q} \to X$	0.03
2_m^+	any	1.4
2_b^+	$gg \to X$	0.9
2_h^+	$gg \to X$	3.1
2_h^-	$gg \to X$	1.7

Fig. 9. – Summary of the expected and observed values for the test-statistic q distributions for the twelve alternative hypotheses tested with respect to the SM Higgs boson. The orange (blue) band represents the 1σ, 2σ, and 3σ around the median expected value for the SM Higgs boson hypothesis (alternative hypothesis). The black point represents the observed value.

In summary, the resonance discovered in July 2012 is clearly visible in the $H \rightarrow ZZ \rightarrow 4\ell$ decay channel, allowing the study of its properties with high precision. The new particle is compatible within uncertainties with a SM Higgs boson with mass $\sim 126\,\text{GeV}$ and alternative spin-parity hypotheses are disfavored by the data. High-mass searches, performed jointly with other final-states channels, show no evidence of other SM-like resonances up to $1\,\text{TeV}$.

REFERENCES

[1] THE ATLAS COLLABORATION, *Phys. Lett. B*, **716** (2012) 1, arXiv:1207.7214 [hep-ex].
[2] THE CMS COLLABORATION, *Phys. Lett. B*, **716** (2012) 30, arXiv:1207.7235 [hep-ex].
[3] THE CMS COLLABORATION, *Phys. Rev. D*892014092007, arXiv:1312.5353 [hep-ex].
[4] BOLOGNESI S., GAO Y., GRITSAN A. V., MELNIKOV K., SCHULZE M., TRAN N. V. and WHITBECK A., *Phys. Rev. D*, **86** (2012) 095031, arXiv:1208.4018 [hep-ph].